International Journal of Nanomedicine

Dovepress
Taylor & Francis Group

Open Access Full Text Article

ORIGINAL RESEARCH

Urinary Extracellular Vesicle Analysis Reveals Early Signs of Kidney Inflammation and Damage in Single Ventricle Paediatric Patients After Fontan Operation

Cristina Grange[1], Luca Deorsola[2,3], Beatrice Degiovanni[2,3], Dario Tomanin[4], Diego Prudente[1], Licia Peruzzi[2,5], Carlo Pace Napoleone[2,3], Benedetta Bussolati[1,4]

[1]Department of Medical Sciences, University of Torino, Torino, Italy; [2]Città della Salute e della Scienza Hospital, Torino, Italy; [3]Pediatric and Congenital Cardiac Surgery, Regina Margherita Children's Hospital, Torino, Italy; [4]Department of Molecular Biotechnology and Health Sciences, University of Torino, Torino, Italy; [5]Pediatric Nephrology Dialysis and Transplant Unit, Regina Margherita Children's Hospital, Torino, Italy

Correspondence: Benedetta Bussolati, Department of Medical Sciences, University of Torino, via Nizza 52, Torino, 10126, Italy, Tel +39011-6706453, Email benedetta.bussolati@unito.it

Background: Extracellular vesicles present in urine (uEVs) are gaining considerable interest as biomarkers, to monitor and predict kidney physio-pathological state. Patients with single ventricle defects and hemodynamic stabilization by Fontan intervention may develop kidney dysfunction as one of the most prevalent extracardiac co-morbidity. Our study aimed to characterize uEVs in children with single ventricle heart defects who underwent Fontan surgery, focusing on markers for monitoring and predicting kidney function, to get physio-pathological insights on possible mechanisms of tissue damage and progression.

Methods: We isolated uEVs from urine of 60 paediatric patients affected by single ventricle defects, and from 10 healthy subjects. We analysed uEVs to assess the presence of the reno-protective hormone Klotho, using super resolution microscopy of single uEVs and ELISA. Moreover, we analysed the levels of markers of kidney regeneration, such as CD133 and CD24, and of inflammation using a bead-based cytofluorimetric multiplex analysis. The markers' levels were correlated with patients' demographical, clinical and surgical data.

Results: uEVs from children with single ventricle defects showed reduced levels of Klotho and CD133, compared with the ones of healthy subjects. In parallel, the levels of inflammatory markers (CD3, CD56, and HLA-DR) were significantly higher. Interestingly, levels of inflammatory markers correlated with age of patients and distance from surgery.

Conclusion: This study demonstrates that single ventricle patients, who underwent Fontan's surgery, present altered levels of uEV biomarkers related to regeneration, inflammation and fibrosis, suggesting the presence of early signs of kidney damage and inflammation, compatible with the complexity of the pathology.

Keywords: urine, exosomes, congenital heart defects, kidney disease, CD133, Klotho

Background

Congenital heart defects affect roughly 1% of newborns. One of the most complex forms of congenital heart disease involves single ventricle physiology.[1,2] Indeed, babies born with single ventricle defects, described by the presence of only one underdeveloped pumping chamber, face some of the most severe heart conditions. Without treatment, their lifespan is often limited.[3] In the 1970s, a revolutionary procedure known as the Fontan surgery emerged. This intervention reroutes blood flow directly to the lungs, alleviating pressure on the compromised ventricular chamber,[1,4] and transforming once-fatal single ventricle congenital heart defects into manageable conditions, with dramatically improvement of patients' outcome.[3] The overall survival rate at 10-, 20-, and 30-year are 74%, 61%, and 43%, respectively.[5,6] While survival rates have seen remarkable progress, these patients still face significant long-term multiorgan adverse complications.[7,8]

Received: 20 June 2024
Accepted: 18 January 2025
Published: 7 May 2025

Graphical Abstract

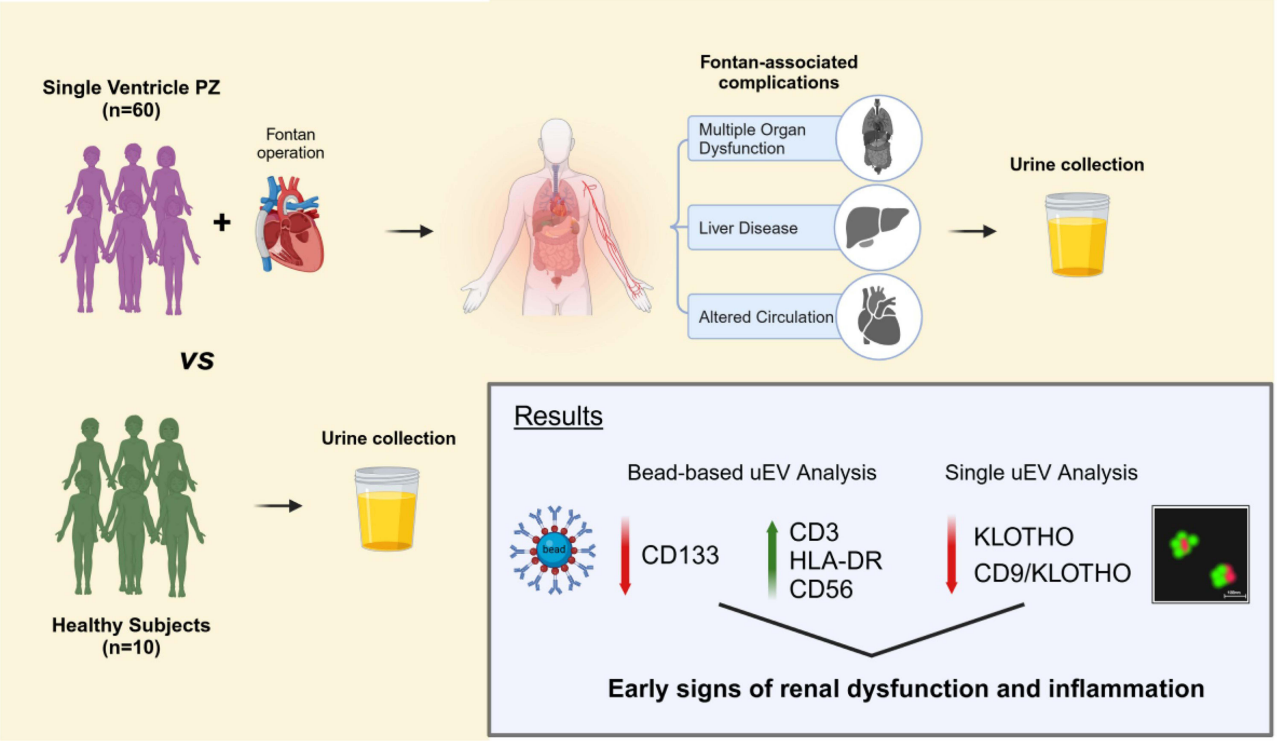

Long-term health problems include chronic inflammation, heart failure, arrhythmias, lymphatic disorders, and mental health challenges.[7,8] Moreover, due to the complexity of the pathology and the increase of life expectancy, kidney dysfunction stands out as one of the most prevalent extracardiac comorbidity in the Fontan population. Hemodynamic derangements after the Fontan operation, as well as acute kidney injury (AKI) episodes after cardiac surgeries, represent the main causes of kidney damage.[5,9] However, information about the progression of renal injury in single ventricle patients after Fontan circulation is limited and, more important, the long-term implications of renal dysfunction are not predictable and well established.[10] In this context, clinical parameters and early biomarkers of renal function may be helpful for patient management and for the direction of therapeutic interventions.

Biological particles in the nanoscale, called extracellular vesicles (EVs) are emerging as a new biomarker category. In fact, EVs' surface markers and cargo (proteins, lipids and different RNA species), may provide information on the pathophysiological state of the originating cell.[11,12] EVs collected into the urine (uEVs) are considered to originate from cells of all segments of the urogenital tract, including kidney, prostate, and bladder as well as by inflammatory infiltrating cells.[13–15] Recent research suggests that most of the uEVs derive from the kidneys.[16] Indeed, the dynamic changes of uEV content may mirror the status of the kidney and several uEV based biomarkers have been proposed.[17] The number itself of uEVs appear to correlate with nephrons' number.[16] Moreover, the expression of glomerular or tubular segment markers indicates a specific cell damage.[14] We previously identified the presence of regenerative/progenitor markers, such as CD133 and SSEA-4, in uEVs of normal subjects, and we showed that their levels were correlated with the prognosis of kidney function in a cohort of transplanted patients.[18] The renal anti-ageing hormone Klotho also appeared to be expressed by uEVs in normal subjects.[19] Of interest, Klotho release is highly modulated during acute and chronic kidney damage.[20–22]

Searching for markers to monitor the pathophysiological status of the kidney in patients affected by congenital heart defects, here we characterized uEVs of 60 single ventricle patients (PZ) subjected to Fontan operation, focusing on the expression of Klotho, an anti-inflammatory and -fibrotic marker, and CD133, a kidney progenitor cell marker,[23–26] and of

inflammatory markers, at single uEV level or as bulk analysis.[18] Results were compared with those obtained in uEVs isolated from healthy paediatric subjects with similar age. Finally, uEV markers were correlated with different clinical parameters and hemodynamic metrics.

Methods

Study Design

All patients enrolled in the present study provided informed written consent for the study. The study protocol was approved by the Bioethics Committee of the A.O.U. Città della Salute e della Scienza Hospital (number 00575/2021, protocol SV001) between 2021 and 2024. The study was conducted according to the principles expressed by the Declaration of Helsinki of 1975, as revised in 2013. The study group was composed of a total of 60 young patients (mean age: 11.3 ± 3.9 years, range: 5.1–18.3 years) affected by single ventricle defects, subjected with Fontan surgery and followed up at the day-hospital of the SC Pediatric Cardiac Surgery and Congenital Heart Disease of Citta della Salute e della Scienza in Torino, Italy. Ten healthy subjects matching for age and sex were also enrolled in the study.

Patients' Urine Collection and uEV Isolation

For each patient, second morning urine (around 10 mL) were collected at the follow up routine medical examination in sterile containers and immediately stored in +4°C and, within 3/4 hours, stored in −80°C after pre-clearing following the recommendations of the Urine Task Force.[13,27] In details, urine samples were centrifuged at 3000 rpm for 15 min to remove cells and other debris. Pre-cleared urine samples were filtered through sequential 0.8, 0.45 and 0.22-nm filters (Merck Millipore, Burlington, MA). Five hundred microliters of pre-cleared urine were stored for MACSplex analysis. uEVs were then collected using sequential ultracentrifugation (Beckman Coulter, OPTIMA L-100 K Ultracentrifuge, Rotor Type 70-Ti, Brea, CA, USA) at 100,000 g for 1 hour at 4°C, as described.[19,28] The pellet was then resuspended in RPMI (Euroclone, Milan, Italy) + 1% DMSO (Merck Millipore) and stored at −80°C until use. For selected experiments, uEVs were obtained from fresh pre-cleared samples obtained within 4 hours from the collection and stored at 4°C. Biochemical analyses were performed by the clinical laboratory of the A.O.U. Città della Salute e della Scienza Hospital in the same day of the urine collection.

Nanoparticle Tracking Analysis

The NanoSight LS300 system (Malvern Panalytical, Malvern, UK) equipped with a 488 nm laser module was used to quantify the EV size and concentration utilizing Nanoparticle Tracking Analysis (NTA) analytical Software, version number 3.2. uEVs from all samples (60 patients and 10 healthy subjects) were diluted (1:200) in sterile saline solution filtered with 0.11 nm pore (Merck Millipore). The following instrument setting was applied: camera level 15, threshold 5 and syringe pump 30. Three videos per sample of 30 seconds were captured. The NTA settings were maintained constant between samples.

Transmission Electron Microscopy

Transmission electron microscopy (TEM) was performed on uEVs, isolated from healthy subjects and Single Ventricle PZ, placed on 200-mesh nickel formvar carbon-coated grids (Electron Microscopy Science) for 20 min to promote adhesion. The grids were then incubated with 2.5% glutaraldehyde plus 2% sucrose. EVs were negatively stained with NanoVan (Nanoprobes, Yaphank, NY, USA) and observed using a Jeol JEM 1400 Flash electron microscope (Jeol, Tokyo, Japan).[29,30]

Super Resolution Microscopy

Super resolution microscopy analyses were performed using Nanoimager S Mark II microscope from ONI (Oxford Nanoimaging, Oxford, UK). The microscope is equipped with a 100x, 1.4NA oil immersion objective, an XYZ closed-loop piezo 736 stage, and dual or triple emission channels split at 640 and 555 nm. For uEV characterization, the EV profiler Kit (ONI) was utilized following manufacturer's protocol. The Kit includes the assay chip, fluorescent antibodies for tetraspanins (anti CD9-488, CD63-568 and CD81-647) and all the buffers and reagents necessary for the experiments. All the experiments were conducted on individual sample, 10 Single Ventricle PZ uEVs and 5 healthy subject uEVs. In addition,

the following antibodies were used: rabbit recombinant monoclonal Klotho antibody (EPR6856, Abcam, Cambridge, UK), Aquaporin 1 (sc-25287, Santa Cruz Biotechnology, Dallas, TX, USA) and Aquaporin 2 (sc-515770, Santa Cruz Biotechnology). The antibodies were conjugated with Alexa Fluor 488, 555 and 647 dyes using the Apex Antibody Labelling Kit (Thermo Fisher Scientific, Waltham, Massachusetts, USA) according to the manufacturer's protocol as described.[31] We used the following combination of antibodies: i) CD9-488, Klotho-555 and CD81-647; ii) Klotho-555, Aquaporin 1–647 and Aquaporin 2–488. The experiments were run in the assay chips present in the EV profiler Kit. Images were taken in dSTORM mode and acquired sequentially in total reflection fluorescence (TIRF) mode. Single-molecule data were filtered using NimOS software (v.1.18.3, ONI). Data has been subsequently analysed with the Collaborative Discovery (CODI) online analysis platform www.alto.codi.bio provided by ONI using the drift correction pipeline version 0.2.3.[29,31]

MACSPlex Exosome Kit Cytofluorimetric Analysis

MACSPlex Exosome Kit (Miltenyi Biotec, Bergisch Gladbach, Germany) allows the analysis of 37 exosomal surface markers and two isotope controls. The antibodies present in the kit are the following: CD3, CD4, CD19, CD8, HLA-DR, CD56, CD105, CD2, CD1c, CD25, CD49e, ROR1, CD209, CD9, SSEA-4, HLA-ABC, CD63, CD40, CD62P, CD11c, CD81, MCSP, CD146, CD41b, CD42a, CD24, CD86, CD44, CD326, CD133-1, CD29, CD69, CD142, CD45, CD31, REA control, CD20, CD14, mIgG1 control. The experiments were performed following the manufacturer's instructions. In details, 15 µL of beads were added to 150 µL of clean urine and the mix was maintained on an orbital rotor overnight at 4°C. The day after, a cocktail of CD9, CD63 and CD81 APC-labelled fluorescent antibodies were added and incubated on orbital rotor for 1 hour at room temperature. After washing, samples were acquired using BD FACSCelesta™ Flow Cytometer (BD Bioscience, NJ, USA). Results were normalized to the mean fluorescence intensity (MFI) of the CD63 tetraspanin that appeared the most consistent among the two experimental groups.[18,32] The experiment was conducted on each individual sample (n: 10 for healthy subjects and 60 for patients).

ELISA for Klotho

An anti-human ELISA (Human soluble a-Klotho code 27998; Immuno-Biological Laboratories) was used to quantify Klotho levels within uEVs, according to the manufacturer's protocol. In detail, single uEV samples isolated from fresh urine of healthy subjects (n = 5) and Single Ventricle PZ (n = 10) were diluted (1:1 v/v) in the resuspension buffer provided in the ELISA. Results were expressed as mean ± SD and normalized per uEV number or per mL of urine.[19]

ELISA for NGAL

For the quantitative determination of human Lipocalin-2 (NGAL) levels in pre-cleared urine was performed using Human Lipocalin-2/NGAL Quantikine ELISA Kit (Cod: DLCN20, from Bio-Techne srl, Milan, Italy) according to manufacturer's protocol. Urine samples were diluted 1:2 in the diluent provided by the kit. At the end of the procedure, the optical density was measured at 450 nm using a microplate reader (Biorad, CA, USA). The experiment was conducted on all samples.

Evaluation of Liver Stiffness

Liver stiffness was evaluated with Transient Hepatic Elastography (Echo-Sens, Paris, France) also known as Fibro-Scan. The probe directs an ultrasound beam (50 hz) through the liver and examines a sample parenchymal volume located 2.5 cm under the skin surface, 1 cm wide and 4 cm long. Assessing ultrasound propagation speed, the device estimates liver stiffness and gives resulting values in kPa (Kilo-Pascal).

Statistical Analysis

GraphPad Prism 8 Software (GraphPad Software Inc., La Jolla, CA, USA) were used for statistical analyses. Results are generally expressed as mean ± SD or ± SEM, as indicated. Normally distributed variables are expressed as mean ± standard deviation (SD) and analyzed by Student's *t*-test. Non-normally distributed variables are expressed as median (interquartile range) and analyzed by Mann–Whitney test or Wilcoxon test, as appropriated. Correlations were evaluated by Pearson's test. Receiver operating characteristics (ROC) curves were analyzed to assess area under the curve (AUC). We only considered AUC values greater than 0.75 for a better power performance.

Results

Patient Description

Sixty patients, affected by single ventricle heart disease were enrolled in the study. All patients had undergone to Fontan surgery in previous years starting from 2001, and, at the time of the study, they were in follow up at the day-hospital of the structure. Ten healthy young subjects with similar age were also enrolled. For each patient, second morning urine samples were collected and pre-analytical factors for handling and storage of samples complied with recommendations of the Urine Task Force[13,27] and International Society for Extracellular Vesicles.[33]

Table 1 summarizes the demographic and clinical information of enrolled patients. No signs of renal dysfunction, as assessed by blood creatinine analysis, performed at the day of urine collection was observed. Creatinine level resulted in the normal range (0.49 ± 0.14 mg/dL). Moreover, urinary NGAL (Neutrophil Gelatinase-Associated Lipocalin) was not increased.[34,35]

uEV Characterization: Exosomal Markers

uEVs of all patients were isolated, following the protocol described in[18,28] in order to analyse their characteristics and markers' expression, in comparison with uEVs isolated from urine of healthy subjects. The study design is summarized in Figure 1. The typical size distribution of small EVs was confirmed using Nanoparticle Tracking Analysis with a mean size of 174.8 nm and 162.5 nm for uEVs isolated from Single Ventricle PZ and healthy subjects, respectively (Figure 2a and b). The uEV concentrations, quantified as particle/mL by NanoSight, were comparable without significant differences between the two experimental groups (17.810^8/mL for Single Ventricle PZ and 22.510^8/mL for healthy subjects) (Figure 2c). TEM analysis revealed uEV integrity and confirmed uEV dimension in the nano range without significant differences among the two groups (50–200nm) (Figure 2d and e).

uEV size, quantified using super resolution microscopy by CODI online analysis platform (www.alto.codi.bio), confirmed similar size among the two groups (Figure 2e). At single EV level, the analysis of CD63, CD81 and CD9, the classical exosomal markers in uEVs, showed heterogeneous expression of single and multiple tetraspanins. In particular, uEVs of both experimental groups, appeared mainly CD9 single positive and CD9/CD63 double positive, whereas CD81 resulted less expressed (Figure 3a). Comparing healthy subjects and Single Ventricle PZ, uEVs isolated from Single Ventricle PZ showed significantly higher level of CD9 (Figure 3a). The analysis of the cumulative expression of each tetraspanin also displayed differences among the two experimental groups, being CD81 significantly more expressed in healthy subject uEVs and CD9 in Single Ventricle PZ uEVs (Figure 3b). On the contrary, the cumulative expression of CD63 was comparable between the two groups (Figure 3b). Representative pictures of the most expressed tetraspanins for each group are shown in Figure 3c.

Table 1 Clinical and Demographic Characteristics of Single Ventricle Patients and Healthy Subjects

Clinical and Demographic Characteristics	Single Ventricle Patients	Healthy Subjects
Number	60	10
Age	11.3±3.9 (5.1–18.3)	8.5 ± 2.5 (6–12)
Sex	37M/23W (61.7%M-38.3%W)	4M/6W (40%M-60%W)
Plasma Creatinine (mg/dL)	0.49±0.14	0.52±0.06
Urine Volume (mL)	8.4±2.1	25.1±1.7
Urine NGAL (ng/mL)	10.0±6.1	18.5±12.8
Distance from Fontan (years)	6.8±4.3 (0.4–14.6)	NA
Liver stiffness (KPa)	13.86±4.24 (6.97–23.57)	NA
Saturation post Fontan (%)	92.74± 6.05 (83–100)	NA

Notes: General information of enrolled patients. No significant differences were observed for plasma creatinine and urine NGAL.
Abbreviation: PZ, patient; M, men; W, women; NGAL, Neutrophil Gelatinase-Associated Lipocalin; NA, not applicable.

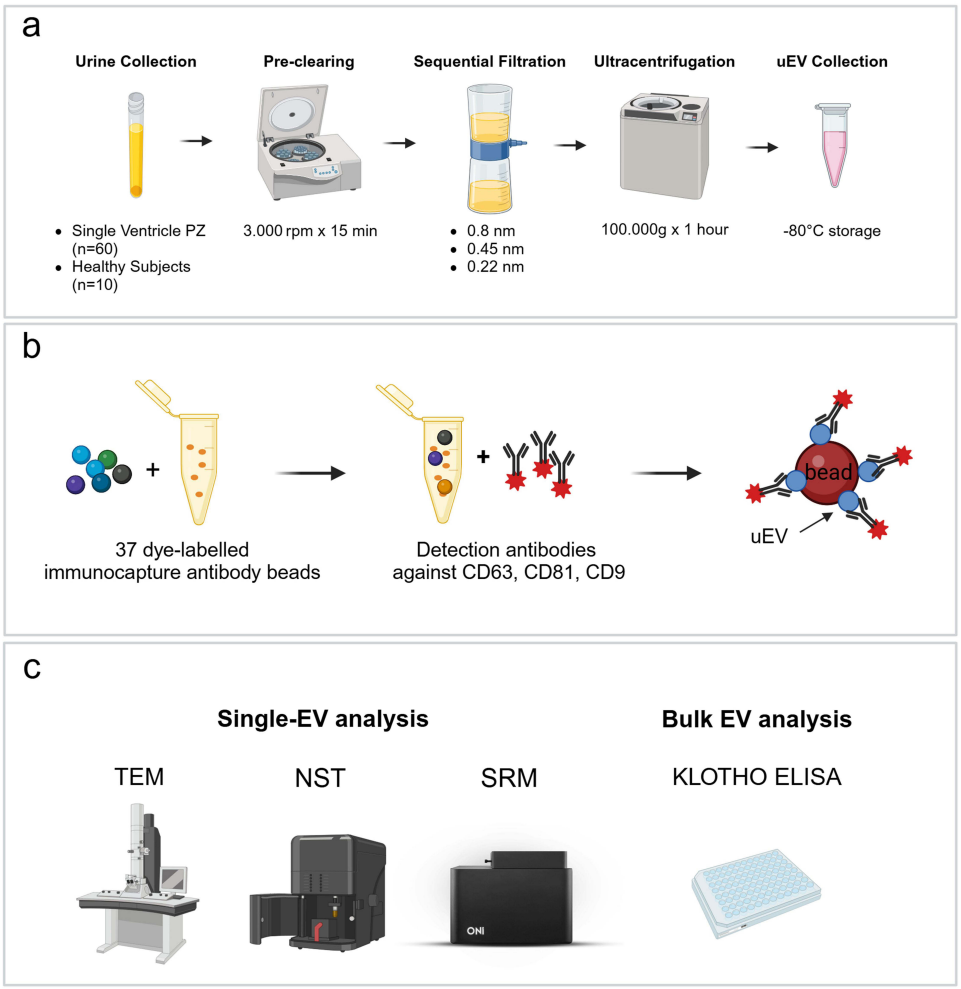

Figure 1 Schematic representation of the study. (**a**) uEV isolation. Representation of the uEV isolation process. (**b**) uEV analysis on pre-cleared urine. Graphical representation of the bead-based uEV analysis, performed on pre-cleared urine samples. (**c**) Isolated uEV analysis. Techniques used for the analyses of isolated uEVs.

Klotho is Reduced in uEVs of Single Ventricle PZ

The renal origin of uEVs was confirmed by the presence of Aquaporin 1 and Aquaporin 2, markers of different nephron segments using super resolution microscopy (Figure 4a–c). We subsequently assessed the presence of Klotho in uEVs; Klotho is a renal hormone involved in protection from fibrosis and aging.[36–38] Klotho positive uEVs appeared as a distinct EV subpopulation, being Aquaporin 1 and Aquaporin 2 co-expression hardly detectable (Figure 4a and Supplementary Figure 1). Comparing the two groups, uEVs from healthy subjects were significantly enriched in Klotho in comparison with those of Single Ventricle PZ (Figure 4a–c). In particular, in healthy subjects, CD9 positive EVs expressed higher Klotho in comparison with Single Ventricle PZ (Figure 4b and c). Single Ventricle PZ uEVs were, at variance, enriched in Aquaporin 2 (Figure 4a).

In addition, Klotho levels were confirmed using the ELISA assay (Figure 4d). uEVs isolated from healthy subjects showed significantly higher level of Klotho compared with Single Ventricle PZ uEVs (817.23 ± 512.07 pg Klotho/10^{11} uEVs for healthy subject vs 160.68 ± 303.34 pg Klotho/10^{11} uEVs for Single Ventricle PZ), normalizing Klotho levels both per uEV number (Figure 4d, left panel) or per mL of sample urine (Figure 4d, right panel).

Evaluation of the Presence of Progenitor and Inflammatory Markers in uEVs

Subsequently, to evaluate possible markers of early signs of renal damage, we assessed the expression level of surface markers related to inflammation and regeneration on uEVs. The MACSplex Kit was used to directly assess 37 different

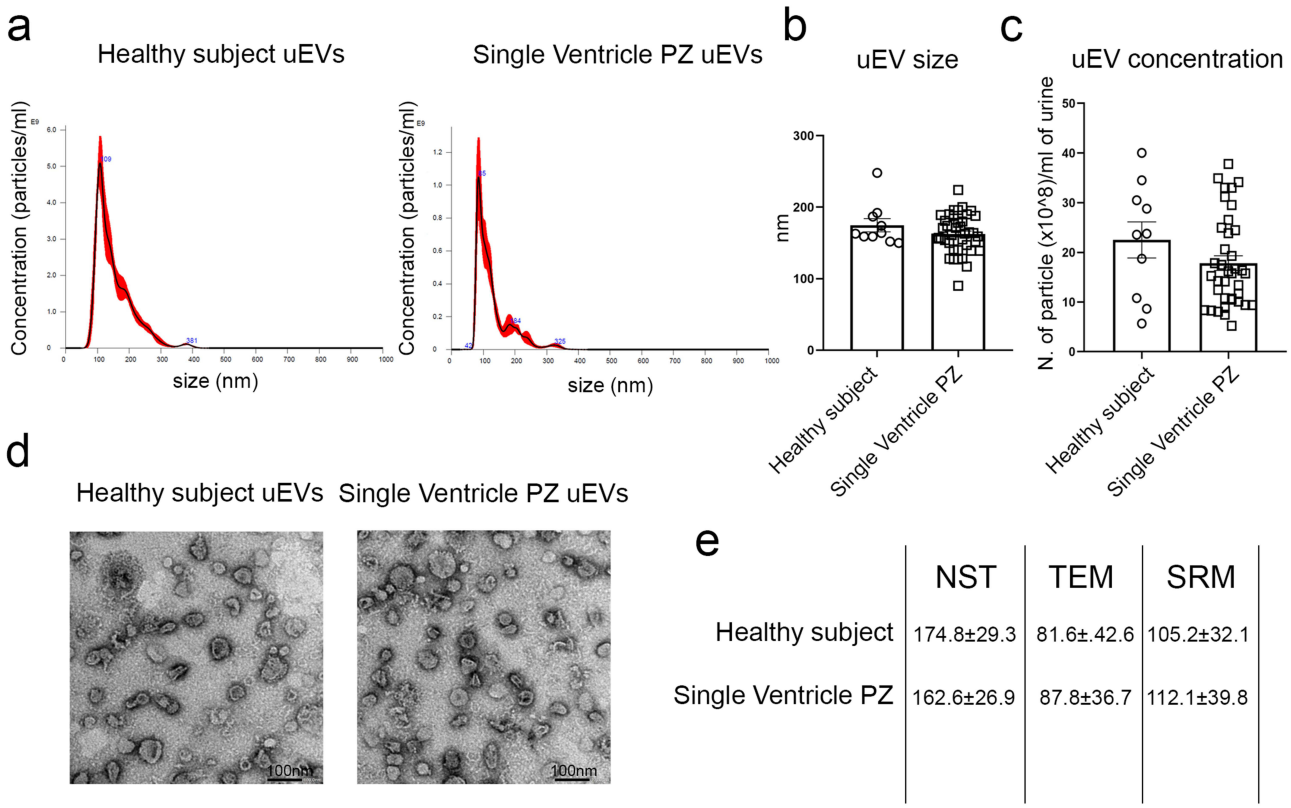

	NST	TEM	SRM
Healthy subject	174.8±29.3	81.6±.42.6	105.2±32.1
Single Ventricle PZ	162.6±26.9	87.8±36.7	112.1±39.8

Figure 2 uEV characterization. (**a**) Representative graphs of Nanoparticle tracking analysis (NTA) of uEVs isolated from urine of healthy subject and Single Ventricle PZ. (**b-c**) Graphs of uEV mean size (**b**) and concentration (**c**) calculated with NanoSight. No significant differences were observed between the two experimental groups. (**d**) Representative TEM images of healthy subject uEVs and Single Ventricle PZ uEVs. (**e**). Description of the mean ±SD of uEV size calculated with NanoSight (NST), TEM and super resolution microscopy (SRM).

surface molecules on pre-cleared urine, and data were normalized to the mean fluorescence intensity of the tetraspanin CD63, which showed comparable levels in the groups as reported ahead (Supplementary Table 1).

The analysis highlighted the presence in both experimental groups of markers related to progenitor cell, renal, epithelial and immune origin (Figure 5). uEVs from healthy subjects showed a homogeneous distribution. The expression levels of inflammatory markers CD3, CD56 and HLA-DR were increased in uEVs isolated from Single Ventricle PZ compared with those from healthy subjects (Figure 5a). On the contrary, uEVs isolated from Single Ventricle PZ expressed at lower levels the progenitor/stem cell marker CD133. In the presence of the renal marker CD24 and the epithelial marker EPCAM was heterogenous in Single Ventricle PZ uEVs (Figure 5b). Sensitivity and specificity of the analysed markers were evaluated with ROC curves, and results are shown in Figure 5c and Supplementary Figure 2. The CD133, CD3 and CD56 values generated an AUC above the 0.75, distinguishing healthy subject uEVs and Single Ventricle PZ uEVs (Figure 5c and Supplementary Table 2).

Clinical Parameters and Marker Correlation

Single values of progenitor, renal and inflammatory markers, obtained with MACSplex kit, were subsequently correlated with demographical, clinical, instrumental and surgical data of Single Ventricle PZ. All the analysed parameters are listed in Table 1 and Supplementary Table 3.

In particular, we observed a significant positive correlation of the inflammatory marker CD3 with the increase of the time post Fontan surgery (Figure 6a). Similarly, the levels of CD3 displayed a significant correlation with the age at the examination, as well as with the increased liver stiffness post Fontan surgery (Figure 6c). A similar trend was observed for the levels of the inflammatory markers HLA-DR and CD56 (Figure 6). On the other side, the renal marker CD24 inversely correlated with the time post Fontan and age (Figure 6a and b). The renal progenitor marker CD133 showed a similar trend, without reaching statistical significance (Figure 6a and b).

https://doi.org/10.2147/IJN.S483534

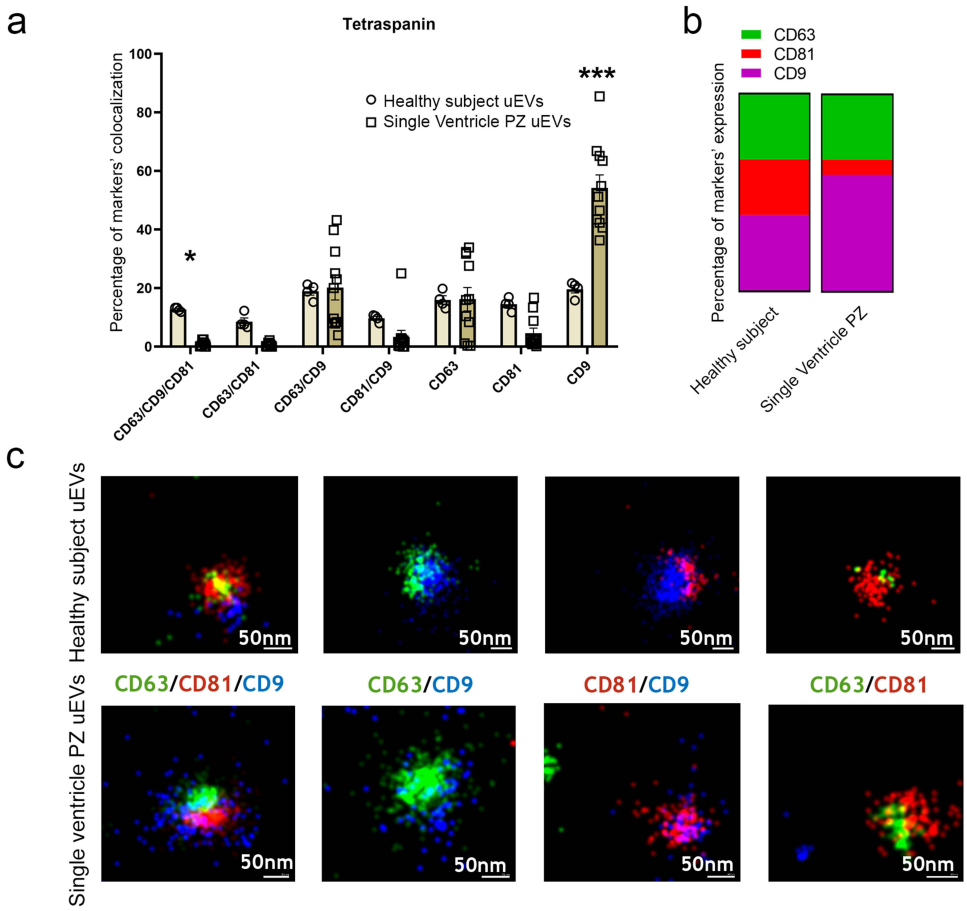

Figure 3 Exosomal markers' characterization. Super resolution microscopy analysis of uEVs. (**a**) The graph shows triple positive, double positive and single positive uEVs for the three tetraspanins (CD63, CD81 and CD9). Data are expressed as percentage of marker's colocalization ±SD; (n=4 healthy subject uEVs and n=10 for Single Ventricle PZ uEVs). *p<0.05 and ***p<0.0001 healthy subject versus Single Ventricle PZ. (**b**) The graph shows the cumulative expression of each tetraspanin (CD63, CD81 and CD9) for healthy subject uEVs and Single Ventricle PZ uEVs. Data are expressed as cumulative percentage of markers' expression. (**c**) Representative super resolution microscopy images of uEVs stained with tetraspanins: CD81 appears in red, CD63 in green, and CD9 in blue. The corresponding scale bar is below each image (scale bar: 50nm).

Analysing the oxygen saturation after Fontan surgery, the level of saturation post-surgery is associated with a reduction of all inflammatory markers (CD3, HLA-DR and CD56) and with an increase of renal and progenitor markers (Supplementary Figure 3).

Discussion

uEVs emerge as attractive candidates for uncovering non-invasive biomarkers in renal diseases. uEVs possess the potential for multiplex analyses, enabling the simultaneous identification of specific pathological processes and their cellular origins. During renal damage, the cargo of uEVs may exhibit alterations, even before the manifestation of changes in conventional serum markers of kidney function, such as blood urea nitrogen (BUN) and creatinine, facilitating earlier disease diagnosis.[15] The present study identifies a unique signature in uEVs isolated from Single Ventricle PZ, possibly underlying early signs of renal alteration. Recent studies have identified the kidney as a primary source of uEVs found in urine.[16] This is supported by proteomic analysis of urinary EVs, which has demonstrated an abundance of renal proteins, such as uromodulin, Aquaporin 1, and Aquaporin 2.[39] These findings suggest that the molecular cargo carried by uEVs holds significant information on the kidney physiopathology. We found that levels of Klotho and CD133, reno-protective and progenitor markers, respectively, were significantly reduced in uEVs from Single Ventricle PZ. In addition, the levels of inflammatory markers CD3, CD56 and HLA-DR appeared significantly increased in uEVs from Single Ventricle PZ and correlated with the extent and complexity of the pathology. Finally, the levels of the exosomal marker CD9 differ between the two experimental groups.

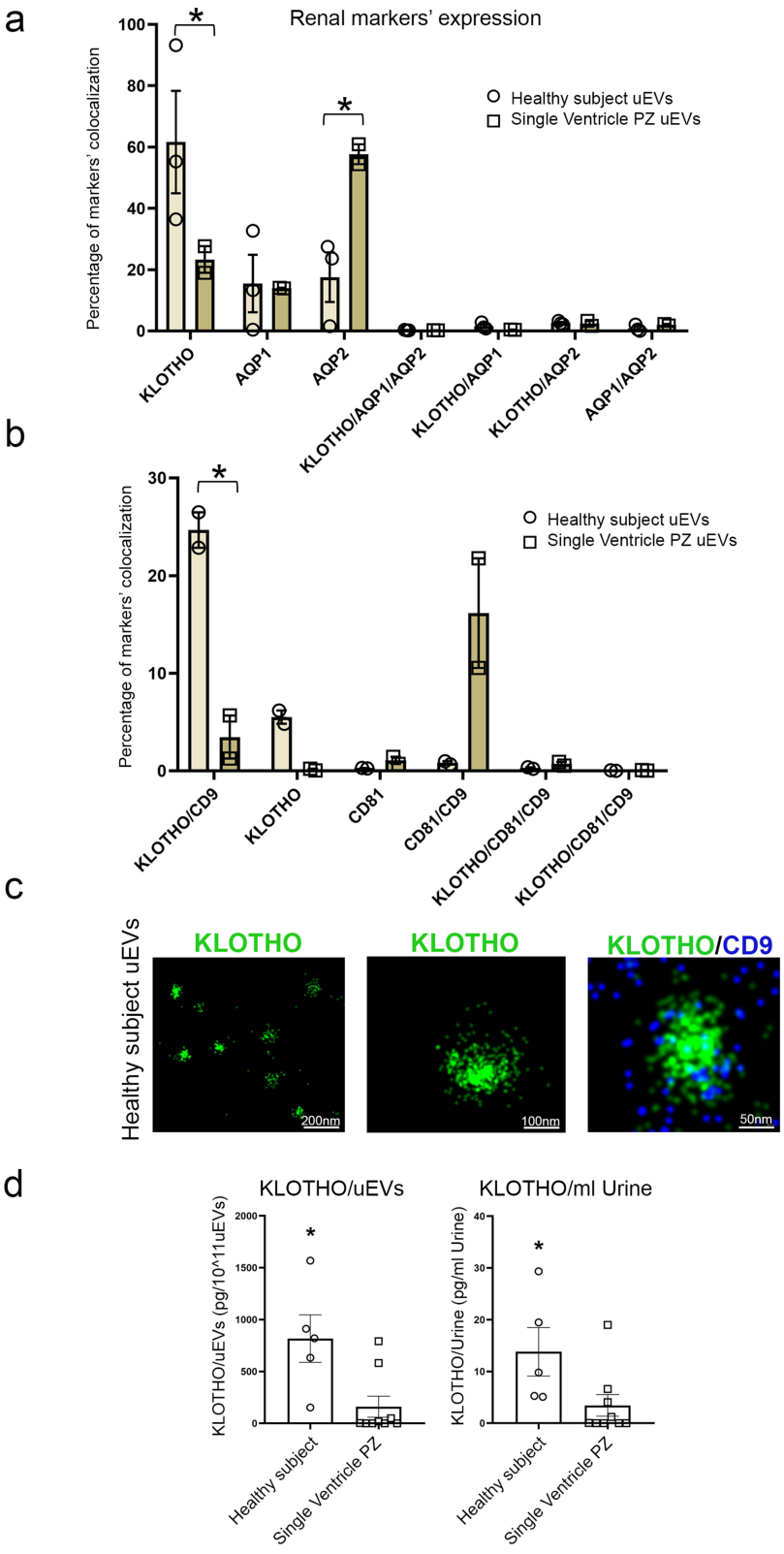

Figure 4 Renal markers' characterization. Super resolution microscopy analysis of uEVs. (**a**) The graph shows triple positive, double positive and single positive uEVs stained with Klotho, Aquaporin 1 (AQP1) and Aquaporin 2 (AQP2) antibodies. Data are expressed as percentage of marker's colocalization ±SD; (n=3 for both conditions). *p<0.05 healthy subject versus Single Ventricle PZ. (**b**) The graph shows triple positive, double positive and single positive uEVs stained with Klotho, CD9 and CD81 antibodies. Data are expressed as percentage of marker's colocalization ±SD; (n=2 for both conditions). *p<0.05 healthy subject versus Single Ventricle PZ. (**c**) Representative super resolution microscopy images of uEVs stained with Klotho and CD9 antibodies. Klotho appears green and CD9 in blue. The corresponding scale bar is below each image. (**d**) Graphs of Klotho levels analysed by ELISA assay. Results are expressed in pg Klotho/10^{11} uEVs (left panel) and pg Klotho/mL of urine (right panel). *p<0.05 healthy subject versus Single Ventricle PZ. (n=5 healthy subject uEVs and n=10 for Single Ventricle PZ uEVs).

https://doi.org/10.2147/IJN.S483534

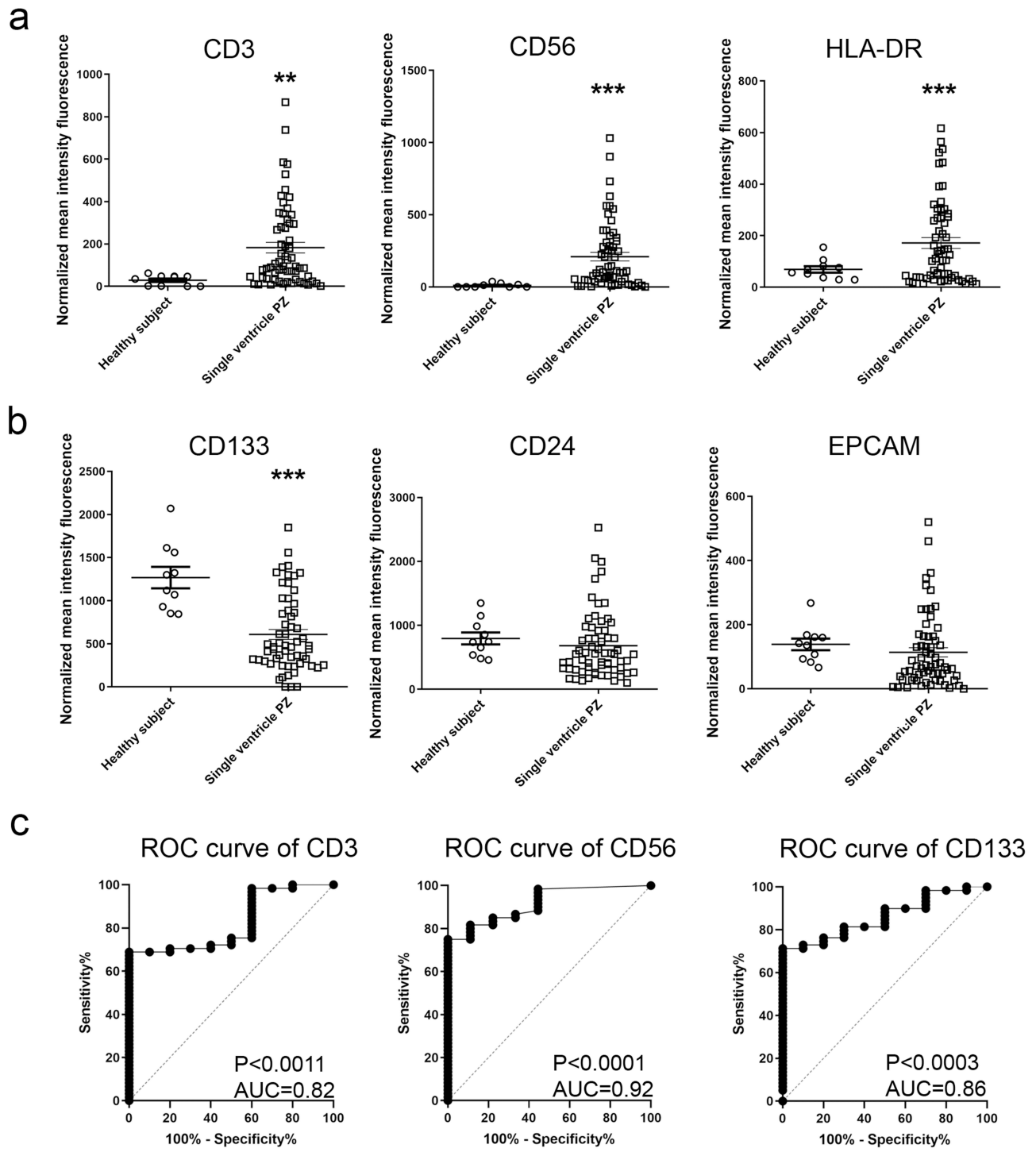

Figure 5 Comparison of progenitor and inflammatory markers in uEVs isolated from healthy subject and Single Ventricle PZ. (**a**) Histograms showing the significantly different inflammatory markers (CD3, CD56 and HLA-DR). (**b**) Histograms illustrating the expression levels of progenitor and epithelial markers (CD133, CD24 and EPCAM). (**c**). Significant ROC curves ($p< 0.75$) of inflammatory (CD3 and CD56) and renal progenitor (CD133) marker. (n=10 healthy subject uEVs and n=60 for Single Ventricle PZ uEVs). Data are expressed as mean fluorescence intensity ±SD, normalized with the fluorescence intensity of CD63. **$p<0.001$ and ***$p<0.0001$ healthy subject versus Single Ventricle PZ.

Recently, several uEV biomarkers of renal injury have been proposed, even if the current data are described in small cohort of patients.[40] During AKI, for example, increased levels of fetuin A and the activating transcription factor 3 (ATF3) mRNA, released by injured tubular cells, were observed in uEVs isolated from AKI patients.[41,42] Moreover, the levels of NGAL present in uEVs has been proposed as better predictor of kidney dysfunction after kidney transplant in

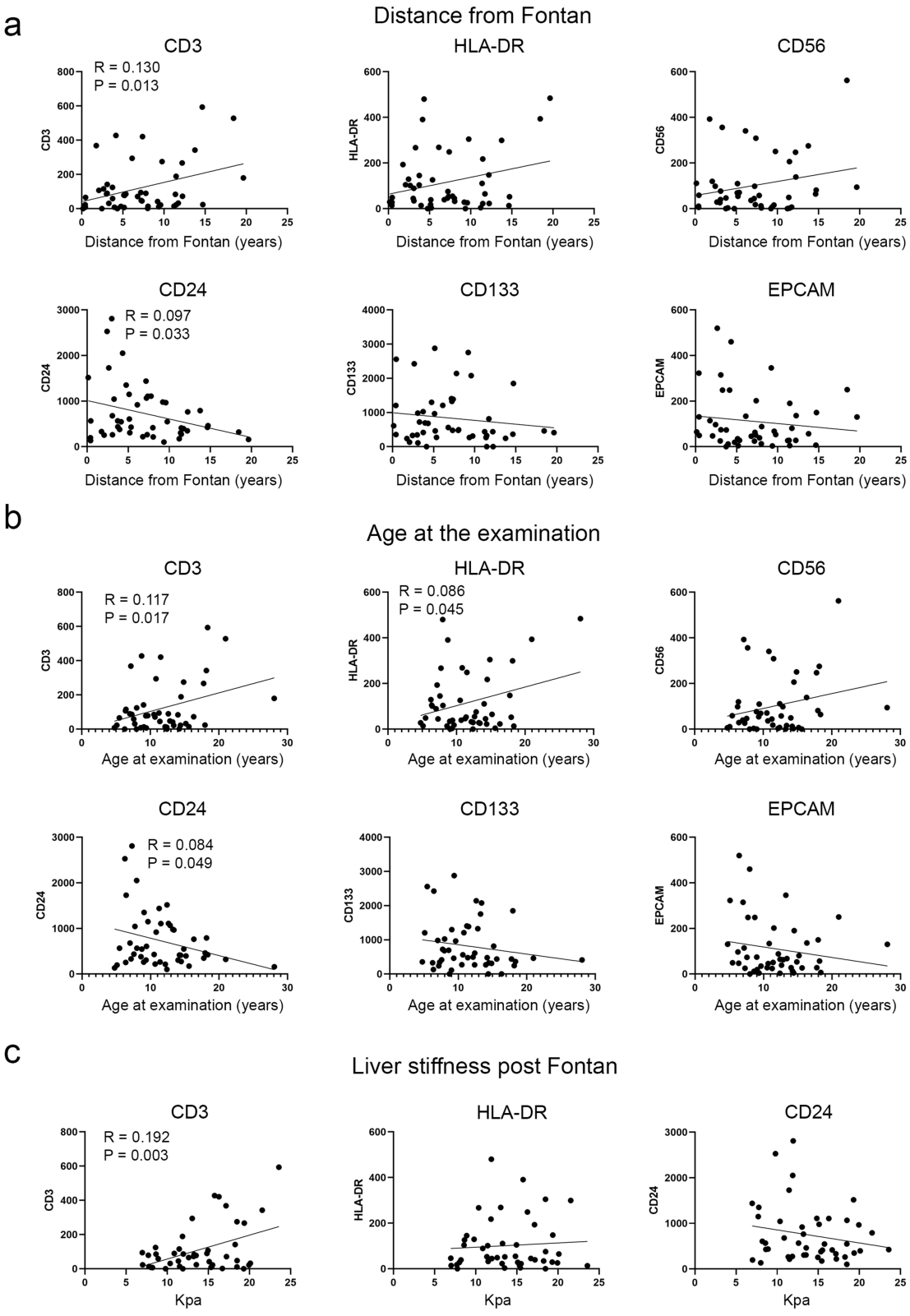

Figure 6 Correlation of surface uEV markers with clinical and surgical parameters. The expression levels of the following EV markers: CD3, HLA-DR, CD56, CD24, CD133 and EPCAM were correlated with the distance from Fontan surgery expressed in years (**a**), the age of patients at examination (**b**) and with the liver stiffness expressed in Kpa (**c**). Correlations were evaluated by Pearson's R test; regression lines with 95% CIs are shown for each correlation.

https://doi.org/10.2147/IJN.S483534

comparison with other urinary non-vesicular markers.[43] In addition, miRNAs carried by uEVs may vary during renal damage, and several miRNAs have been proposed as biomarkers of renal fibrosis such as miRNA-29c, miRNA-200b.[44] Of interest, in cases of glomerular injury, podocytes may release detectable uEVs in urine. Podocyte-specific proteins such as Wilms' tumor 1 protein have been proposed as specific biomarkers for focal segmental glomerulosclerosis in mouse and human studies.[42,45]

Patients with congenital single ventricle defect undergoing Fontan surgery present a unique pathophysiological state characterized by chronically diminished cardiac output with elevated systemic venous pressure, absence of phasic flow in the systemic venous district and of pulsatile flow in the pulmonary circulation. During time, it has become evident that this hemodynamic derangement is one of the factors involved in a progressive phenomenon of multiorgan failure.[7] Historically, the first described complications were heart failure, pulmonary hypertension, and, particularly, the couple Protein Losing Enteropathy - Plastic Bronchitis, both identified under the common definition of "Failing Fontan" and depending on a lymphatic overload.[46] However, in the last decade, the spectrum of Fontan related adverse effects has gradually widened with the discovery of hepatic and renal damage, which have been object of a huge series of studies.[7,8] Although they represent prevalent complications and may exhibit progressive worsening over time,[47,48] there are no early biomarkers available for the monitoring of the disease progression and related complications.

Therefore, we first assessed the level of the renal hormone Klotho, an aging suppressor, which acts as a humoral modulator of diverse cellular processes encompassing antioxidative and anti-inflammatory mechanisms.[23,49] Dysregulation of Klotho is common in renal dysfunction, but may also contribute to the pathogenesis of different diseases such as aging, fibrosis, bone disorder and vascular calcification.[24,50–55] We previously showed that, in normal subjects, uEVs carry Klotho.[19] Of interest, we here better characterized Klotho-positive uEVs, identifying a distinct uEV subpopulation not expressing the tubular markers Aquaporin 1 or Aquaporin 2. The present study highlighted the reduction of Klotho in uEVs of Single Ventricle PZ, compared to the levels of healthy subjects, using different techniques, suggesting the impairment of the endocrine renal function of Klotho. The observed Klotho reduction in urinary EVs could possibly correlate with its decreased level in the circulation, with consequent increase of systemic oxidative stress, as well as with signs of early aging. Indeed, early osteoporosis, liver fibrosis, slow conduction speed and alteration of coagulation are commonly observed in these patients.[7,56] Circulating levels of Klotho in these patients deserve further studies.

Moreover, increased uEV levels of CD3, CD56 and HLA-DR in Single Ventricle PZ indicated the presence of signs of inflammation. Considering that circulating EVs in plasma do not cross the glomerular barrier,[16,39] the identification of EVs from inflammatory cells in urine indicates the presence of renal tissue inflammation, a hallmark of kidney acute and chronic diseases. Renal inflammatory cells, activated during damage, may contribute to the release of EVs into the urine. In turn, EVs specifically released by damaged renal resident cells may sustain renal inflammation.[57] In this study, the presence of uEVs expressing inflammatory markers, highlighting the presence of inflammatory cells within the kidney tissue, correlated with age and time after Fontan surgery. This is in line with the presence of systemic inflammation in patients with congenital single ventricle which has been reported in different studies[7,48] either by evaluating circulating proinflammatory cytokines such as TNF-α, interleukin-6, by estimating spleen size[58] or by assessing tissue inflammatory markers. In particular, in patient with Fontan associated liver disease, RNA sequencing of liver biopsies exhibited upregulation of pathways related to inflammation.[48]

Another uEV marker that appears interesting is CD133, as its levels were observed reduced in uEVs from paediatric patients with acute and chronic glomerulonephritis[59,60] and correlated with kidney function in transplanted patients.[18] In paediatric Single Ventricle PZ, the uEV level of CD133 was also significantly reduced, suggesting a renal specific impairment in the ability to kidney repair after damage. It is in fact reported that renal dysfunction may appear when patients reach adolescence, and its incidence increase with adulthood.[47] In addition, AKI occurs in up to 40% of patients after Fontan surgery.[61] Recent evidence shows that even one episode of AKI changes the risk of developing long-term kidney problems such as chronic kidney disease.[62–65] Finally, CD24, a specific marker of renal uEVs,[66] appeared to inversely correlate with age and time after Fontan surgery, suggesting that it might represent a general renal decline due to reduced nephron number or renal cell-EV release.

The precise monitoring of kidney function in Single Ventricle PZ is of great importance, to counteract the decline since the beginning. However, Single Ventricle PZ have low muscle mass that influence serum creatine;[7] and for this reason, creatinine base equations overestimate the GFR and cannot be accurate indicator of renal functionality.[10] In our cohort, accordingly, the plasma creatinine and urinary NGAL did not show abnormalities. Indeed, kidney dysfunction is common in young adults, at a later stage than that of our patients.[67] Our study highlights the presence of early changes in uEV markers in children with Single Ventricle defects, without clinical manifestations of kidney damage, and well correlates with the inflammatory and pro-fibrotic alterations, characteristic of this pathology.

Conclusions

In conclusion, data presented here identify a distinct phenotype of uEVs isolated from Single Ventricle PZ highlighting abnormal levels of inflammatory markers and decreased level of regenerative and anti-fibrotic markers, mirroring the pathological condition of these patients. The present study opens a new way to use urine for monitoring renal status and comorbidities related to the complexity of Fontan circulation. This method offers several advantages: it's minimally invasive and a promise as a point-of-care testing tool. A validation study with an independent subjects' cohort will be instrumental to confirm these results.

Abbreviations

AKI, Acute Kidney Injury; AQP, Aquaporin; BUN, Blood Urea Nitrogen; NGAL, Human Lipocalin-2; NST, NanoSight; PZ, Patient; TEM, Transmission Electron Microscopy.

Data Sharing Statement

The data and results analysed during the current study are available from the corresponding author upon reasonable request.

Ethics Approval and Consent to Participate

The study was conducted according to the principles expressed by the Declaration of Helsinki of 1975, as revised in 2013. The study protocol was approved by the Bioethics Committee of the A.O.U. Città della Salute e della Scienza Hospital (number 00575/2021, protocol SV001).

Consent for Publication

All authors have agreed to publish this manuscript.

Acknowledgments

We acknowledge the technical support of Dr. Massimo Cedrino and of Prof. Giovanni Camussi for electron microscopy.

Author Contributions

All authors made a significant contribution to the work reported, whether that is in the conception, study design, execution, acquisition of data, analysis and interpretation, or in all these areas; took part in drafting, revising or critically reviewing the article; gave final approval of the version to be published; have agreed on the journal to which the article has been submitted; and agree to be accountable for all aspects of the work.

Funding

C.G. and B.B are member of the Urine Task Force unit, a team of ISEV experts that provide recommendations to improve reproducibility of EV research.

Disclosure

The authors declare that they have no competing interests. Part of the results of this manuscript were presented in the abstract submitted for Kidney Week 2024 ASN conference, (SA-PO918).

References

1. Gilbert K, Forsch N, Hegde S, et al. Atlas-based computational analysis of heart shape and function in congenital heart disease. *J Cardiovasc Transl Res*. 2018;11(2):123–132. doi:10.1007/s12265-017-9778-5
2. Khairy P, Poirier N, Mercier LA. Univentricular heart. *Circulation*. 2007;115(6):800–812. doi:10.1161/CIRCULATIONAHA.105.592378
3. Erikssen G, Liestøl K, Aboulhosn J, et al. Preoperative versus postoperative survival in patients with univentricular heart: a nationwide, retrospective study of patients born in 1990-2015. *BMJ Open*. 2023;13(7):e069531. doi:10.1136/bmjopen-2022-069531
4. Fontan F, Baudet E. Surgical repair of tricuspid atresia. *Thorax*. 1971;26(3):240–248. doi:10.1136/thx.26.3.240
5. Pujol C, Schiele S, Maurer SJ, et al. Patients with single-ventricle physiology over the age of 40 years. *J Clin Med*. 2020;9(12):1–8. doi:10.3390/jcm9124085
6. Downing TE, Allen KY, Glatz AC, et al. Long-term survival after the Fontan operation: twenty years of experience at a single center. *J Thorac Cardiovasc Surg*. 2017;154(1):243–253.e2. doi:10.1016/j.jtcvs.2017.01.056
7. Ritmeester E, Veger VA, van der Ven JPG, et al. Fontan circulation associated organ abnormalities beyond the heart, lungs, liver, and gut: a systematic review. *Front Cardiovasc Med*. 2022;9:826096. doi:10.3389/fcvm.2022.826096
8. Hedlund E, Lundell B. Fontan circulation has improved life expectancy for infants born with complex heart disease over the last 50 years but has also resulted in significant morbidity. *Acta Paediatr*. 2022;111(1):11–16. doi:10.1111/apa.16023
9. Zafar F, Lubert AM, Katz DA, et al. Long-term kidney function after the Fontan operation. *J Am Coll Cardiol*. 2020;76(3):334–341. doi:10.1016/j.jacc.2020.05.042
10. Muraoka M, Nagata H, Yamamura K, et al. Long-term renal involvement in association with Fontan circulation. *Pediatr Cardiol*. 2024;45(2):340–350. doi:10.1007/s00246-023-03334-3
11. Wiklander OPB, Brennan MÁ, Lötvall J, Breakefield XO, El Andaloussi S. Advances in therapeutic applications of extracellular vesicles. *Sci Transl Med*. 2019;11(492):eaav8521. doi:10.1126/scitranslmed.aav8521
12. van Niel G, Carter DRF, Clayton A, Lambert DW, Raposo G, Vader P. Challenges and directions in studying cell-cell communication by extracellular vesicles. *Nat Rev Mol Cell Biol*. 2022;23(5):369–382. doi:10.1038/s41580-022-00460-3
13. Erdbrügger U, Blijdorp CJ, Bijnsdorp IV, et al. Urinary extracellular vesicles: a position paper by the urine task force of the international society for extracellular vesicles. *J Extracell Vesicles*. 2021;10(7):e12093. doi:10.1002/jev2.12093
14. Erdbrügger U, Hoorn EJ, Le TH, Blijdorp CJ, Burger D. Extracellular Vesicles in Kidney Diseases: moving Forward. *Kidney360*. 2023;4(2):245–257. doi:10.34067/KID.0001892022
15. Grange C, Bussolati B. Extracellular vesicles in kidney disease. *Nat Rev Nephrol*. 2022;18(8):499–513. doi:10.1038/s41581-022-00586-9
16. Blijdorp CJ, Hartjes TA, Wei K-Y, et al. Nephron mass determines the excretion rate of urinary extracellular vesicles. *J Extracell Vesicles*. 2022;11(1):e12181. doi:10.1002/jev2.12181
17. Grange C, Dalmasso A, Cortez JJ, Spokeviciute B, Bussolati B. Exploring the role of urinary extracellular vesicles in kidney physiology, aging, and disease progression. *Am J Physiol Cell Physiol*. 2023;325(6):C1439–C1450. doi:10.1152/ajpcell.00349.2023
18. Burrello J, Monticone S, Burrello A, et al. Identification of a serum and urine extracellular vesicle signature predicting renal outcome after kidney transplant. *Nephrol Dial Transplant*. 2023;38(3):764–777. doi:10.1093/ndt/gfac259
19. Grange C, Papadimitriou E, Dimuccio V, et al. Urinary extracellular vesicles carrying Klotho improve the recovery of renal function in an acute tubular injury model. *Mol Ther*. 2020;28(2):490–502. doi:10.1016/j.ymthe.2019.11.013
20. Kim HR, Nam BY, Kim DW, et al. Circulating α-klotho levels in CKD and relationship to progression. *Am J Kidney Dis*. 2013;61(6):899–909. doi:10.1053/j.ajkd.2013.01.024
21. Donate-Correa J, Matos-Perdomo E, González-Luis A, et al. The value of Klotho in kidney transplantation. *Transplantation*. 2023;107(3):616–627. doi:10.1097/TP.0000000000004331
22. Wang Q, Su W, Shen Z, Wang R. Correlation between Soluble α-Klotho and renal function in patients with chronic kidney disease: a review and meta-analysis. *Biomed Res Int*. 2018;9481475. doi:10.1155/2018/9481475
23. Fu Y, Cao J, Wei X, Ge Y, Su Z, Yu D. Klotho alleviates contrast-induced acute kidney injury by suppressing oxidative stress, inflammation, and NF-KappaB/NLRP3-mediated pyroptosis. *Int Immunopharmacol*. 2023;118:110105. doi:10.1016/j.intimp.2023.110105
24. Shimamura Y, Hamada K, Inoue K, et al. Serum levels of soluble secreted α-Klotho are decreased in the early stages of chronic kidney disease, making it a probable novel biomarker for early diagnosis. *Clin Exp Nephrol*. 2012;16(5):722–729. doi:10.1007/s10157-012-0621-7
25. Bussolati B, Moggio A, Collino F, et al. Hypoxia modulates the undifferentiated phenotype of human renal inner medullary CD133+ progenitors through Oct4/miR-145 balance. *Am J Physiol Renal Physiol*. 2012;302(1):F116–28. doi:10.1152/ajprenal.00184.2011
26. Aggarwal S, Grange C, Iampietro C, Camussi G, Bussolati B. Human $CD133^{+}$ renal progenitor cells induce erythropoietin production and limit fibrosis after acute tubular injury. *Sci Rep*. 2016;6(1):37270. doi:10.1038/srep37270
27. van Royen ME, Soekmadji C, Grange C, et al. The quick reference card "Storage of urinary EVs" - A practical guideline tool for research and clinical laboratories. *J Extracell Vesicles*. 2023;12(3):e12286. doi:10.1002/jev2.12286
28. Dimuccio V, Bellucci L, Genta M, et al. Upregulation of miR145 and miR126 in EVs from renal cells undergoing EMT and urine of diabetic nephropathy patients. *Int J Mol Sci*. 2022;23(20):12098. doi:10.3390/ijms232012098
29. Skovronova R, Grange C, Dimuccio V, Deregibus MC, Camussi G, Bussolati B. Surface marker expression in small and medium/large mesenchymal stromal cell-derived extracellular vesicles in naive or apoptotic condition using orthogonal techniques. *Cells*. 2021;10(11):2948. doi:10.3390/cells10112948
30. Bruno S, Chiabotto G, Cedrino M, et al. Extracellular vesicles derived from human liver stem cells attenuate chronic kidney disease development in an in vivo experimental model of renal ischemia and reperfusion injury. *Int J Mol Sci*. 2022;23(3):1485. doi:10.3390/ijms23031485
31. Gebara N, Scheel J, Skovronova R, et al. Single extracellular vesicle analysis in human amniotic fluid shows evidence of phenotype alterations in preeclampsia. *J Extracell Vesicles*. 2022;11(5):e12217. doi:10.1002/jev2.12217
32. Tassinari S, D'Angelo E, Caicci F, et al. Profile of matrix-entrapped extracellular vesicles of microenvironmental and infiltrating cell origin in decellularized colorectal cancer and adjacent mucosa. *J Extracell Biol*. 2024;3(3):e144. doi:10.1002/jex2.144
33. Welsh JA, Goberdhan DCI, O'Driscoll L, et al. Minimal information for studies of extracellular vesicles (MISEV2023): from basic to advanced approaches. *J Extracell Vesicles*. 2024;13(2):e12404. doi:10.1002/jev2.12404

34. Schinstock CA, Semret MH, Wagner SJ, et al. Urinalysis is more specific and urinary neutrophil gelatinase-associated lipocalin is more sensitive for early detection of acute kidney injury. *Nephrol Dial Transplant*. 2013;28(5):1175–1185. doi:10.1093/ndt/gfs127
35. Yamamoto A, Nakayama S, Wakabayashi Y, Yoshino Y, Kitazawa T. Urine neutrophil gelatinase-associated lipocalin as a biomarker of adult pyelonephritis. *J Infect Chemother*. 2023;29(5):508–512. doi:10.1016/j.jiac.2023.01.001
36. Hu MC, Kuro-o M, Moe OW. Secreted klotho and chronic kidney disease. *Adv Exp Med Biol*. 2012;728:126–157. doi:10.1007/978-1-4614-0887-1_9
37. Hu MC, Kuro-o M, Moe OW. Renal and extrarenal actions of Klotho. *Semin Nephrol*. 2013;33(2):118–129. doi:10.1016/j.semnephrol.2012.12.013
38. Satoh M, Nagasu H, Morita Y, Yamaguchi TP, Kanwar YS, Kashihara N. Klotho protects against mouse renal fibrosis by inhibiting Wnt signaling. *Am J Physiol Renal Physiol*. 2012;303(12):F1641–51. doi:10.1152/ajprenal.00460.2012
39. Gonzales PA, Pisitkun T, Hoffert JD, et al. Large-scale proteomics and phosphoproteomics of urinary exosomes. *J Am Soc Nephrol*. 2009;20 (2):363–379. doi:10.1681/ASN.2008040406
40. Svenningsen P, Sabaratnam R, Jensen BL. Urinary extracellular vesicles: origin, role as intercellular messengers and biomarkers; efficient sorting and potential treatment options. *Acta Physiol*. 2020;228(1):e13346. doi:10.1111/apha.13346
41. Zhou H, Pisitkun T, Aponte A, et al. Exosomal Fetuin-A identified by proteomics: a novel urinary biomarker for detecting acute kidney injury. *Kidney Int*. 2006;70(10):1847–1857. doi:10.1038/sj.ki.5001874
42. Zhou H, Cheruvanky A, Hu X, et al. Urinary exosomal transcription factors, a new class of biomarkers for renal disease. *Kidney Int*. 2008;74 (5):613–621. doi:10.1038/ki.2008.206
43. Alvarez S, Suazo C, Boltansky A, et al. Urinary exosomes as a source of kidney dysfunction biomarker in renal transplantation. *Transplant Proc*. 2013;45(10):3719–3723. doi:10.1016/j.transproceed.2013.08.079
44. Lv LL, Cao YH, Ni HF, et al. MicroRNA-29c in urinary exosome/microvesicle as a biomarker of renal fibrosis. *Am J Physiol Renal Physiol*. 2013;305(8):F1220–7. doi:10.1152/ajprenal.00148.2013
45. Kwon SH, Woollard JR, Saad A, et al. Elevated urinary podocyte-derived extracellular microvesicles in renovascular hypertensive patients. *Nephrol Dial Transplant*. 2017;32(5):800–807. doi:10.1093/ndt/gfw077
46. Ghanayem NS, Berger S, Tweddell JS. Medical management of the failing Fontan. *Pediatr Cardiol*. 2007;28(6):465–471. doi:10.1007/s00246-007-9007-0
47. Rychik J, Atz AM, Celermajer DS, et al. American heart association council on cardiovascular disease in the young and council on cardiovascular and stroke nursing. evaluation and management of the child and adult with Fontan circulation: a scientific statement from the American heart association. *Circulation*. 2019;140(6):e234–e284. doi:10.1161/CIR.0000000000000696
48. Bravo-Jaimes K, Wu X, Reardon LC, et al. Intrahepatic transcriptomics differentiate advanced fibrosis and clinical outcomes in adults with the Fontan circulation. *J Am Coll Cardiol*. 2024;83(7):726–738. doi:10.1016/j.jacc.2023.12.005
49. Wang YY, Lin YH, Wu VC, et al. Decreased Klotho expression causes accelerated decline of male fecundity through oxidative injury in murine testis. *Antioxidants*. 2023;12(9):1671. doi:10.3390/antiox12091671
50. Kuro-O M. Klotho and endocrine fibroblast growth factors: markers of chronic kidney disease progression and cardiovascular complications? *Nephrol Dial Transplant*. 2019;34(1):15–21. doi:10.1093/ndt/gfy126
51. Liu L, Jia J, Cheng X, Gao S, Yan T. The optimal cut-off values of Klotho for predicting all-cause and cardiovascular mortality among chronic kidney disease: results from NHANES. *Sci Rep*. 2024;14(1):4647. doi:10.1038/s41598-024-52701-4
52. Martín-Vírgala J, Martín-Carro B, Fernández-Villabrille S, et al. Soluble Klotho, a potential biomarker of chronic kidney disease-mineral bone disorders involved in healthy ageing: lights and shadows. *Int J mol Sci*. 2024;25(3):1843. doi:10.3390/ijms25031843
53. Tsujikawa H, Kurotaki Y, Fujimori T, Fukuda K, Nabeshima Y. Klotho, a gene related to a syndrome resembling human premature aging, functions in a negative regulatory circuit of vitamin D endocrine system. *Mol Endocrinol*. 2003;17(12):2393–2403. doi:10.1210/me.2003-0048
54. Koh N, Fujimori T, Nishiguchi S, et al. Severely reduced production of klotho in human chronic renal failure kidney. *Biochem Biophys Res Commun*. 2001;280(4):1015–1020. doi:10.1006/bbrc.2000.4226
55. Zhang X, Li L, Tan H, et al. Klotho-derived peptide 1 inhibits cellular senescence in the fibrotic kidney by restoring Klotho expression via posttranscriptional regulation. *Theranostics*. 2024;14(1):420–435. doi:10.7150/thno.89105
56. Tomkiewicz-Pajak L, Hoffman P, Trojnarska O, Lipczyńska M, Podolec P, Undas AJ. Abnormalities in blood coagulation, fibrinolysis, and platelet activation in adult patients after the Fontan procedure. *Thorac Cardiovasc Surg*. 2014;147(4):1284–1290. doi:10.1016/j.jtcvs.2013.06.011
57. Kim R, Kim TM. The role of extracellular vesicles in kidney disease progression. *Kidney Res Clin Pract*. 2024. doi:10.23876/j.krcp.24.201
58. de Santiago ER, Téllez L, Garrido-Lestache Rodríguez-Monte E, et al. Fontan protein-losing enteropathy is associated with advanced liver disease and a proinflammatory intestinal and systemic state. *Liver Int*. 2020;40(3):638–645. doi:10.1111/liv.14375
59. Dimuccio V, Peruzzi L, Brizzi MF, et al. Acute and chronic glomerular damage is associated with reduced CD133 expression in urinary extracellular vesicles. *Am J Physiol Renal Physiol*. 2020;318(2):F486–F495. doi:10.1152/ajprenal.00404.2019
60. Dimuccio V, Ranghino A, Praticò Barbato L, et al. Urinary CD133+ extracellular vesicles are decreased in kidney transplanted patients with slow graft function and vascular damage. *PLoS One*. 2014;9(8):e104490. doi:10.1371/journal.pone.0104490
61. Sammour F, Haw M, Paisey J, et al. Renal function of patients with a failing Fontan circuit undergoing total cavopulmonary revision surgery. *Pediatr Cardiol*. 2009;30(3):282–288. doi:10.1007/s00246-008-9344-7
62. Mammen C, Al Abbas A, Skippen P, et al. Long-term risk of CKD in children surviving episodes of acute kidney injury in the intensive care unit: a prospective cohort study. *Am J Kidney Dis*. 2012;59(4):523–530. doi:10.1053/j.ajkd.2011.10.048
63. Coca SG, Yusuf B, Shlipak MG, Garg AX, Parikh CR. Long-term risk of mortality and other adverse outcomes after acute kidney injury: a systematic review and meta-analysis. *Am J Kidney Dis*. 2009;53(6):961–973. doi:10.1053/j.ajkd.2008.11.034
64. See EJ, Jayasinghe K, Glassford N, et al. Long-term risk of adverse outcomes after acute kidney injury: a systematic review and meta-analysis of cohort studies using consensus definitions of exposure. *Kidney Int*. 2019;95(1):160–172. doi:10.1016/j.kint.2018.08.036
65. Madsen NL, Goldstein SL, Frøslev T, Christiansen CF, Olsen M. Cardiac surgery in patients with congenital heart disease is associated with acute kidney injury and the risk of chronic kidney disease. *Kidney Int*. 2017;92(3):751–756. doi:10.1016/j.kint.2017.02.021
66. Keller S, Rupp C, Stoeck A, et al. CD24 is a marker of exosomes secreted into urine and amniotic fluid. *Kidney Int*. 2007;72(9):1095–1102. doi:10.1038/sj.ki.5002486
67. Van den Eynde J, Westenberg JJM, Hazekamp MG, et al. Noninvasive advanced cardiovascular magnetic resonance-derived Fontan hemodynamics are associated with reduced kidney function but not albuminuria. *J Am Heart Assoc*. 2024;13(3):e033122. doi:10.1161/JAHA.123.033122